bonds in the cis position (labeled S–F$_a$). Thus, the primary substitution effect dominates, and Δ is negative. The secondary effect cannot be fully active, since angle relaxation as expected from the VSEPR model is prevented by the ring formation. The predicted sequence in bond angles would be NSN > NSF > FSF, while the actual sequence is NSF (NSF$_e$ = 97.3°, NSF$_a$ = 91.4°) > FSF (F$_e$SF$_a$ = 88.6°, F$_e$SF$_e$ = 91.7°) > NSN (80.7°). The average S–F bond length (1.568 Å) is slightly longer than the bonds in SF$_6$ (1.562 (1) Å).[31] A very similar substitution effect is observed for $(SeF_4O)_2$[19] and $(TeF_4O)_2$,[19] where the Se–F and Te–F bonds trans to oxygen are shorter than the cis bonds by 0.030 (16) and 0.046 (16) Å, respectively.

Acknowledgment. Support by the Deutsche Forschungsgemeinschaft and the Fonds der Chemie is gratefully acknowledged.

Registry No. $(ClNSF_4)_2$, 79593-52-5.

Supplementary Material Available: A listing of total scattering intensities (2 pages). Ordering information is given on any current masthead page.

---

(31) C. H. Holder, D. Gregory, and M. Fink, *J. Chem. Phys.*, **75**, 5318 (1981).

Contribution from the Department of Chemistry,
Harvard University, Cambridge, Massachusetts 02138

Synthesis and Stereochemistry of Metal(II) Thiolates of the Types $[M(SR)_4]^{2-}$, $[M_2(SR)_6]^{2-}$, and $[M_4(SR)_{10}]^{2-}$ (M = Fe(II), Co(II))†

KARL S. HAGEN and R. H. HOLM*

Received May 24, 1983

Examples of the homoleptic binuclear Fe(II) and Co(II) thiolates of the type $[M_2(SR)_6]^{2-}$ (RS = EtS, S$_2$-*o*-xyl (*o*-xylene-α,α'-dithiolate)) have been synthesized and structurally characterized by X-ray diffraction methods. The following results were obtained (space group; crystal parameters; Z; unique data ($I > 3\sigma(I)$); R/R_w). $(Et_4N)_2[Fe_2(SEt)_6]$ (**1**): $P2_1/n$; a = 9.815 (2) Å, b = 14.588 (2) Å, c = 14.791 (3) Å, β = 100.97 (2)°; 2; 1980; 4.3/4.8. $(Et_4N)_2[Fe_2(S_2\text{-}o\text{-xyl})_3]\cdot 2MeCN$ (**2**): $P2_1/n$; a = 10.62 (1) Å, b = 25.06 (1) Å, c = 18.927 (8) Å, β = 101.94 (6)°; 4; 2042; 6.6/6.9. $(n\text{-}Bu_4N)_2[Co_2(SEt)_6]$ (**3**): *Pbca*; a = 16.672 (7) Å, b = 21.017 (5) Å; c = 33.849 (6) Å; 8; 3067; 6.2/6.1. $(Et_4N)_2[Co_2(SEt)_6]$ (**4**): $P2_1/n$; a = 9.829 (2) Å, b = 14.504 (4) Å, c = 14.772 (4) Å, β = 100.90 (2)°; 2; 1961; 4.7/5.3. All anions are edge-shared imperfect tetrahedral dimers in which the S–M–S and the M–S–M angles of the $M_2(\mu\text{-}S)_2$ bridges are respectively smaller (97–102°) and larger (78–81°) than the values of 109.5 and 70.5° for a perfect tetrahedral dimer. Compounds **1** and **4** are isomorphous and contain centrosymmetric anions with planar bridge units having the anti configuration of ethyl groups. The anion **2** exists in one of several possible isomeric forms and contains one terminal chelate ring and two others furnishing one bridging and one terminal sulfur atom. This connectivity requires an anti bridge unit, which is nonplanar. When crystallized as compound **3**, the anion is stabilized in the syn form with a nonplanar bridge unit. Other structural features of **1**–**4** are described. In acetonitrile solution the equilibrium $3[M_2(SEt)_6]^{2-} \rightleftharpoons 2[M(SEt)_4]^{2-} + [M_4(SEt)_{10}]^{2-}$ (M = Fe(II), Co(II)) was identified by use of ^1H NMR spectra; $K_{eq}(Co) >> K_{eq}(Fe)$. Salts of the new complexes $[Co(SEt)_4]^{2-}$ and $[M_4(SEt)_{10}]^{2-}$ were synthesized in order to identify equilibrium components. The equilibrium was further substantiated by a structure determination of $(Me_4N)_2[Fe_4(SEt)_{10}]$. This compound crystallizes in space group *Pbca* with a = 18.879 (4) Å, b = 24.981 (5) Å, c = 21.599 (4) Å, and Z = 8. On the basis of 2928 unique data ($I > 3\sigma(I)$) the structure was refined to R = 4.6% and R_w = 4.8%. The anion contains a $Fe_4(\mu\text{-}S)_6$ adamantane-like cage and is the ninth M(II)–thiolate complex shown to possess this stereochemistry and the first with alkylthiolate ligands. The chemistry of Fe(II) thiolates is now known to encompass tetrahedral $[Fe(SR)_4]^{2-}$, edge-shared tetrahedral $[Fe_2(SR)_6]^{2-}$, cyclic $[Fe_3(SR)_3X_6]^{2-}$, and cage $[Fe_4(SR)_{10}]^{2-}$, all of which have (distorted) tetrahedral Fe(II) sites. No complexes of higher nuclearity have been detected nor have other structural forms of those with nuclearities of one to four.

Introduction

Assembly of the biologically relevant clusters $[Fe_nS_n(SR)_4]^{2-}$[1] (n = 2,4) in reaction systems containing Fe(II, III) salts, thiolate, and elemental sulfur has been demonstrated to proceed via the intermediacy of the Fe(II)–thiolate complexes $[Fe(SR)_4]^{2-}$ and $[Fe_4(SR)_{10}]^{2-}$.[2] Reaction sequences have been delineated in some detail for the R = Ph case. More recently it has been shown that strongly reducing $[Fe(SEt)_4]^{2-}$ in reactions with sulfur in acetonitrile affords $[Fe_2S_2(SEt)_4]^{2-}$, $[Fe_3S_4(SEt)_4]^{3-}$, and $[Fe_6S_9(SEt)_2]^{4-}$.[3,4] Because the first of these can be converted to $[Fe_4S_4(SEt)_4]^{2-}$ by being heated in acetonitrile, $[Fe(SEt)_4]^{2-}$ serves as a common precursor to all known structural types of Fe–S–SR clusters of synthetic origin except those that appear to require a bidentate thiolate ligand for formation.[5] These observations have led to a systematic investigation of Fe(II)–thiolate chemistry in the form of reactions 1–4[3] in Figure 1. Variation of the RS$^-$:Fe(II) mole ratio affords the product complexes **1**–**4** whose compositions conform to these ratios. Examples of **1**–**4** have been isolated as quaternary ammonium or phosphonium salts.[2-4,8-14] The

---

† Whereas it is the policy of *Inorganic Chemistry* to publish (in full papers and notes) all crystal structure coordinates, this procedure has been modified in the case of multiple crystal structure determinations. In such cases, certain crystal structure data will be placed in the supplementary material.

(1) Berg, J. M.; Holm, R. H. In "Metal Ions in Biology"; Spiro, T. G., Ed.; Wiley-Interscience: New York, 1982; Vol. 4, Chapter 1.

(2) Hagen, K. S.; Reynolds, J. G.; Holm, R. H. *J. Am. Chem. Soc.* **1981**, *103*, 4054.

(3) Hagen, K. S.; Holm, R. H. *J. Am. Chem. Soc.* **1982**, *104*, 5496.

(4) Hagen, K. S.; Watson, A. D.; Holm, R. H. *J. Am. Chem. Soc.* **1983**, *105*, 3905.

(5) These are the Fe(II) complexes $[Fe_3S(S_2\text{-}o\text{-xyl})_3]^{2-}$[6] (S$_2$-*o*-xyl = *o*-xylene-$\alpha,\alpha'$-dithiolate) and a ring-methylated derivative[7] of the same structure.

(6) Hagen, K. S.; Christou, G.; Holm, R. H. *Inorg. Chem.* **1983**, *22*, 309.

(7) Henkel, G.; Tremel, W.; Krebs, B. *Angew. Chem., Int. Ed. Engl.* **1981**, *20*, 1033.

0020-1669/84/1323-0418$01.50/0

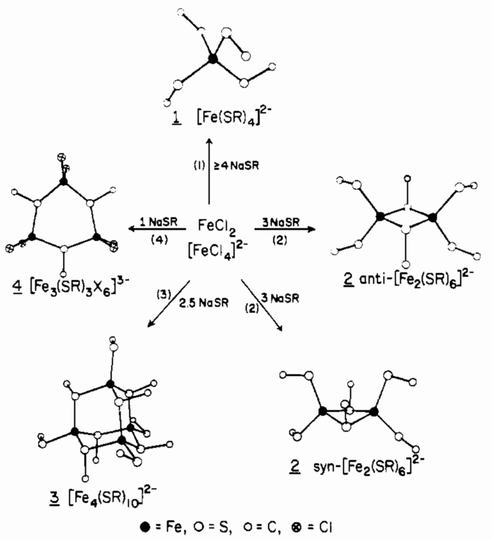

Figure 1. Reactions of iron(II) chloride with 1–4 equiv of NaSR. The structures of products **1**–**4** are schematically illustrated; all but the syn form of **2** have been isolated.

mononuclear tetrahedral species **1** are represented by $[Fe(SPh)_4]^{2-}$,[2,8-10] $[Fe(SEt)_4]^{2-}$,[3,4] and $[Fe(S_2\text{-}o\text{-}xyl)_2]^{2-}$.[14] The first apparent example of an isolated binuclear complex **2** was $[Fe_2(S_2\text{-}o\text{-}xyl)_3]^{2-}$;[13,14] however, its structure was not determined at the time. Several examples of the tetranuclear complex **3** have been prepared.[2,11,12] Of these, $[Fe_4(SPh)_{10}]^{2-}$, containing the adamantane-like $Fe_4(\mu\text{-}S)_6$ cage,[2,11,12] is the most thoroughly characterized. The trinuclear cyclic species **1** is exemplified by $[Fe_3(SPh)_3Cl_6]^{3-}$.[3] The only other discrete iron thiolates known are the Fe(III) species of the types $[Fe(SR)_4]^-$ ($[Fe(S_2\text{-}o\text{-}xyl)_2]^-$,[13,14] $[Fe(S\text{-}2,3,5,6\text{-}Me_4C_6H)_4]^-$[15]) and $[Fe_2(SR)_8]^{2-}$ ($[Fe_2(edt)_4]^{2-}$[16,17] (edt = 1,2-ethanedithiolate)).

With investigations of the synthesis and structural and electronic properties and reactions of types **1** and **3** complexes being substantially complete, attention has been directed to those of type **2**. Reported here are the structure of $[Fe_2(S_2\text{-}o\text{-}xyl)_3]^{2-}$ and the preparations and structures of $[Fe_2(SEt)_6]^{2-}$ and $[Fe_4(SEt)_{10}]^{2-}$. Also included is corresponding information for the analogous Co(II) complexes $[Co_2(SEt)_6]^{2-}$ and $[Co_4(SEt)_{10}]^{2-}$ and for $[Co(SEt)_4]^{2-}$. Characterization of the latter complex and the two $[M_4(SEt)_{10}]^{2-}$ species was required in order to identify an unexpected reaction of both $[M_2(SEt)_6]^{2-}$ complexes in solution. The only molecular Co(II) thiolates isolated prior to this work were several tetrahedral species of the $[Co(SR)_4]^{2-}$ type[8,14,18-20] and the prototype cage complex $[Co_4(SPh)_{10}]^{2-}$.[21] The synthesis, properties, and reactions of type **4** complexes will be described in full elsewhere.

Experimental Section

Preparation of Compounds. All operations were performed under a pure dinitrogen or argon atmosphere (<2 ppm of dioxygen). Sodium ethanethiolate was prepared from sodium and ethanethiol in THF. The white solid was collected by filtration, washed with ether, and dried in vacuo. $(Et_4N)_2[Fe(SEt)_4]$ was prepared as described.[4]

Iron(II) Compounds. (a) $(Et_4N)_2[Fe_2(SEt)_6]$. To a slurry of 3.80 g (30 mmol) of anhydrous $FeCl_2$ and 4.97 (30 mmol) of Et_4NCl in 100 mL of propionitrile was added 7.57 g (90 mmol) of NaSEt in small portions, causing formation of a dark orange-brown solution. The solution was stirred overnight and was filtered to remove NaCl. The solid was washed with 2 × 10 mL of acetonitrile, and the filtrate and washings were combined. Ether (~50 mL) was added, and the solution was kept at −25 °C overnight. The product (8.6 g, 78%) was obtained as large orange-brown crystals after it was collected, washed with 5% v/v acetonitrile/ether, and dried in vacuo. Anal. Calcd for $C_{28}H_{70}Fe_2N_2S_6$: C, 45.51; H, 9.54; Fe, 15.11; N, 3.79; S, 26.03. Found: C, 45.65; H, 9.32; Fe, 15.22; N, 3.96; S, 25.65.

(b) $(Me_4N)_2[Fe_4(SEt)_{10}]$. A solution of 125 mmol of NaSEt (from 2.87 g of sodium and 9.30 mL of thiol) in 75 mL of methanol was added to a slurry of 8.14 g (50 mmol) of $FeCl_2\cdot 2H_2O$ and 2.74 g (25 mmol) of Me_4NBr in 50 mL of methanol. The dark yellow-brown solution was stirred for 2 h and condensed to an oil, which was treated with 50 mL of 2-propanol. Sodium halides were removed by filtration, and the flask containing the filtrate was connected by a U-tube to another containing ~125 mL of ether. After 2 days the product was collected, washed with ether, and dried in vacuo; large brown crystals were obtained (6.5 g, 53%). Anal. Calcd for $C_{28}H_{74}Fe_4N_2S_{10}$: C, 34.21; H, 7.59; Fe, 22.73; N, 2.85; S, 32.62. Found: C, 34.35; H, 7.65; Fe, 22.84; N, 2.87; S, 32.74.

Cobalt(II) Compounds. (a) $(Me_4N)_2[Co(SEt)_4]$. To a slurry of 4.03 g (48 mmol) of NaSEt in ~75 mL of acetonitrile were added 2.63 g (24 mmol) of Me_4NCl and 1.30 g (10 mmol) of anhydrous $CoCl_2$. After being stirred for 3 h, the pale blue slurry was filtered to remove NaCl. The solid was washed with 2 × 10 mL of acetonitrile, the filtrate and washings were combined, and the resultant mixture was reduced in volume until incipient crystallization at ~45 °C. Slow cooling of this solution to 4 °C gave after 18 h large deep blue needles, which were collected, washed with ether, and dried in vacuo (2.0 g, 44%). A second crop was afforded by addition of ether to the filtrate. Anal. Calcd for $C_{16}H_{44}CoN_2S_4$: C, 42.54; H, 9.82; Co, 13.05; N, 6.20; S, 28.39. Found: C, 41.02; H, 9.54; Co, 12.97; N, 6.59; S, 29.32.

(b) $(Et_4N)_2[Co_4(SEt)_{10}]$ and (c) $(Et_4N)_2[Co_2(SEt)_6]$. A slurry of 1.30 g (10 mmol) of $CoCl_2$ in ~75 mL of acetonitrile was treated with 2.52 g (30 mmol) of NaSEt. To the deep green solution was added 1.65 g (10 mmol) of Me_4NCl, and the mixture was stirred for 1 h. After NaCl was removed by filtration and the solid was washed with 2 × 10 mL of acetonitrile, the filtrate and washings were combined and the volume was reduced by ~50% in vacuo. An equal volume of ether was added, and the mixture was cooled to −25 °C. An amorphous red solid was removed by filtration. Addition of 25 mL of ether and cooling to −25 °C caused separation of large, dark green blocks. These were collected, washed with ether, and dried in vacuo (1.7 g (23%) of $(Et_4N)_2[Co_4(SEt)_{10}]$ was obtained). Anal. Calcd for $C_{36}H_{90}Co_4N_2S_{10}$: C, 39.10; H, 8.27; Co, 21.30; N, 2.56; S, 28.94. Found: C, 39.87; H, 7.92; Co, 20.35; N, 2.52; S, 27.85. Upon cooling of the filtrate to which the ether washings in the last step were added, large dark green needles formed. These were collected, washed with ether, and dried in vacuo (2.0 g (27%) of $(Et_4N)_2[Co_2(SEt)_6]$ was obtained). Anal. Calcd for $C_{28}H_{70}Co_2N_2S_6$: C, 45.11; H, 9.47; Co, 15.81; N, 3.81; S, 25.81. Found: C, 45.07; H, 9.28; Co, 15.86; N, 3.68; S, 25.58. X-ray analysis has shown that this salt contains the anti form of the anion.

(d) $(n\text{-}Bu_4N)_2[Co_2(SEt)_6]$. To a slurry of 6.80 g (75 mmol) of NaSEt in 100 mL of acetonitrile were added 3.25 g (25 mmol) of anhydrous $CoCl_2$ and 8.05 g (25 mmol) of $n\text{-}Bu_4NCl$. The deep green

---

(8) Holah, D. G.; Coucouvanis, D. *J. Am. Chem. Soc.* **1975**, *97*, 6917.

(9) Coucouvanis, D.; Swenson, D.; Baenziger, N. C.; Holah, D. G.; Kostikas, A.; Simopoulos, A.; Petrouleas, V. *J. Am. Chem. Soc.* **1976**, *98*, 5721.

(10) Coucouvanis, D.; Swenson, D.; Baenziger, N. C.; Murphy, C.; Holah, D. G.; Sfarnas, N.; Simopoulos, A.; Kostikas, A. *J. Am. Chem. Soc.* **1981**, *103*, 3350.

(11) Hagen, K. S.; Berg, J. M.; Holm, R. H. *Inorg. Chim. Acta* **1980**, *45*, L17.

(12) Hagen, K. S.; Stephan, D. W.; Holm, R. H. *Inorg. Chem.* **1982**, *21*, 3928.

(13) Lane, R. W.; Ibers, J. A.; Frankel, R. B.; Holm, R. H. *Proc. Natl. Acad. Sci. U.S.A.* **1975**, *72*, 2868.

(14) Lane, R. W.; Ibers, J. A.; Frankel, R. B.; Papaefthymiou, G. C.; Holm, R. H. *J. Am. Chem. Soc.* **1977**, *99*, 84.

(15) Millar, M.; Lee, J. F.; Koch, S. A.; Fikar, R. *Inorg. Chem.* **1982**, *21*, 4105.

(16) Herskovitz, T.; DePamphilis, B. V.; Gillum, W. O.; Holm, R. H. *Inorg. Chem.* **1975**, *14*, 1426.

(17) Snow, M. R.; Ibers, J. A. *Inorg. Chem.* **1973**, *12*, 249.

(18) Beck, W.; Stetter, K. H.; Tadrus, S.; Schwarzhans, K. E. *Chem. Ber.* **1967**, *100*, 3944.

(19) Hollebone, B. R.; Nyholm, R. S. *J. Chem. Soc. A* **1971**, 332.

(20) Swenson, D.; Baenziger, N. C.; Coucouvanis, D. *J. Am. Chem. Soc.* **1978**, *100*, 1932.

(21) (a) Dance, I. G.; Calabrese, J. C. *J. Chem. Soc., Chem. Commun.* **1975**, 762. (b) Dance, I. G. *J. Am. Chem. Soc.* **1979**, *101*, 6264.

Table I. Crystallographic Data for $(Et_4N)_2[Fe_2(SEt)_6]$ (A), $(Et_4N)_2[Fe_2(S_2\text{-}o\text{-}xyl)_3]\cdot 2MeCN$ (B), $(n\text{-}Bu_4N)_2[Co_2(SEt)_6]$ (C), $(Et_4N)_2[Co_2(SEt)_6]$ (D), and $(Me_4N)_2[Fe_4(SEt)_{10}]$ (E)

	A	B	C	D	E
formula	$C_{28}H_{70}Fe_2N_2S_6$	$C_{44}H_{70}Fe_2N_4S_6$	$C_{44}H_{86}Co_2N_2S_6$	$C_{28}H_{70}Co_2N_2S_6$	$C_{28}H_{74}Fe_4N_2S_{10}$
mol wt	738.95	959.15	969.57	745.13	982.89
a, Å	9.815 (2)	10.62 (1)	16.672 (7)	9.829 (2)	18.879 (4)
b, Å	14.588 (2)	25.06 (1)	21.017 (5)	14.504 (4)	24.981 (5)
c, Å	14.791 (3)	18.927 (8)	33.849 (6)	14.772 (4)	21.599 (4)
β, deg	100.97 (2)	101.94 (6)		100.90 (2)	
V, Å^3	2079.0 (6)	4929 (6)	11 860 (6)	2068 (1)	10 186 (4)
cryst syst	monoclinic	monoclinic	orthorhombic	monoclinic	orthorhombic
space group	$P2_1/n$	$P2_1/n$	$Pbca$	$P2_1/n$	$Pbca$
d_{calcd}, g/cm^3	1.18	1.29	1.29	1.20	1.28
d_{obsd}, g/cm^3	1.18 (1)	d	1.29 (1)	1.20 (1)	1.29 (1)
Z	2	4	8	2	8
radiation			Mo Kα (λ = 0.710 69 Å)		
abs coeff (μ), cm^{-1}	10.1	8.7	7.9	11.1	15.0
cryst size, mm	0.22 × 0.39 × 0.50	0.16 × 0.32 × 0.40	0.34 × 0.54 × 0.60	0.55 × 0.40 × 0.60	0.20 × 0.24 × 0.50
scan speed,[b] deg/min	2.0–29.3	2.9–29.3	2.9–29.3	2.9–29.3	2.9–29.3
scan range,[c] deg	1.4	2.0	1.8	2.0	2.0
bkgd/scan time ratio	0.33	0.25	0.25	0.25	0.25
data colled	$+h, +k, \pm l$ $(3.0° \leq 2\theta \leq 45°)$	$+h, +k, \pm l$ $(3.0° \leq 2\theta \leq 40°)$	$\pm h, +k, +l$ $(3.0° \leq 2\theta \leq 40°)$	$\pm h, +k, +l$ $(3.0° \leq 2\theta \leq 48°)$	$+h, +k, +l$ $(3.0° \leq 2\theta \leq 43°)$
no. of unique data ($I > 3\sigma(I)$)	1980	2042	3067	1961	2928
R_{merg}[e]	0.0116	0.0993	0.0315	0.0250	0.0505
no. of variables	229	379	529	208	397
GOF[a]	1.50	1.32	1.42	1.24	1.19
R, %	4.3	6.6	6.2	4.7	4.6
R_w, %	4.8	6.9	6.1	5.3	4.8

[a] GOF = $[\Sigma w(|F_o| - |F_c|)^2/(n_o - n_v)]^{1/2}$, where n_o and n_v are the number of data and variables, respectively. [b] $\theta/2\theta$ scan. [c] Scan range, $x + (2\theta_{K\alpha_2} - 2\theta_{K\alpha_1})$. [d] Not measured. [e] $R_{merg} = [\Sigma N_i \Sigma_{j=1}^{N_i}(\bar{F}_j - F_j)^2/\Sigma(N_i - 1)\Sigma_{j=1}^{N_i}F_j^2]^{1/2}$, where N_i is the number of equivalent reflections in a given set, F_j is one member of the set, and $\bar{F}_j$ is the mean.

solution was stirred for 1 h, and NaCl was removed by filtration. The solid was washed with 2 × 10 mL of acetonitrile, and the filtrate and washings were combined. The volume of the solution was reduced by ~50%. Addition of 50 mL of ether followed by cooling at −25 °C overnight caused separation of dark green crystals. These were collected, washed twice with 5% v/v acetonitrile/ether, and dried in vacuo (6.3 g, 52%). This material was not analyzed but was identified by X-ray analysis to be $(n\text{-}Bu_4N)_2[Co_2(SEt)_6]$, containing the syn form of the anion.

Collection and Reduction of X-ray Data. Single crystals were obtained as follows: $(Et_4N)_2[Fe_2(SEt)_6]$, slow cooling of a propionitrile/ether solution to −25 °C; $(Et_4N)_2[Fe_2(S_2\text{-}o\text{-}xyl)_3]\cdot 2MeCN$, slow cooling of a concentrated acetonitrile solution of the unsolvated compound;[13,22] $(Et_4N)_2[Co_2(SEt)_6]$, preparative procedure; $(n\text{-}Bu_4N)_2[Co_2(SEt)_6]$, slow cooling of an acetonitrile/ether solution to −25 °C; $(Me_4N)_2[Fe_4(SEt)_{10}]$, layering ether on a concentrated propionitrile solution. All cyrstals were mounted in glass capillaries that were sealed under argon. Diffraction experiments were performed at ~25 °C on a Nicolet R3m four-circle diffractometer with a Mo X-ray source equipped with a graphite monochromator. The crystal and machine parameters used in the unit cell determination and data collection are summarized in Table I. All intensity data were collected by the $\theta/2\theta$ technique. The intensities of three check reflections were measured every 123 reflections during data collection. The only significant decay was found with compound B data, which were corrected for an 8% intensity decay. The SHELXTL programs XTAPE and XEMP were used for data processing and empirical absorption correction, respectively. The latter was applied to all data sets. Maximum and minimum transmission factors are 0.794 and 0.620 for B, 0.518 and 0.487 for C, and 0.786 and 0.733 for D.

Structure Solution and Refinement. The SHELXTL program package (Nicolet XRD Corp., Fremont, CA) was used throughout. Heavy-atom positions were revealed by the direct-methods program SOLV. All remaining non-hydrogen atoms were located by using successive difference Fourier maps and blocked-cascade least-squares refinement. Atomic scattering factors were taken from the tabulation of Cromer and Waber.[23] In the last stage of refinement, fixed contributions were included from hydrogen atoms with a C–H distance of 0.96 Å and thermal parameters set at 1.2 times that of the bonded carbon atom. Unique data used in the refinements and final R factors are given in Table I. Atom coordinates of anions are compiled in Tables II–IV.[24] Refinements of individual structures are briefly described.

(a) $(Et_4N)_2[Fe_2(SEt)_6]$. The systematic absences $h0l$ ($h + l = 2n + 1$) and $0k0$ ($k = 2n + 1$) uniquely define the space group $P2_1/n$ (nonstandard setting of $P2_1/c$ No. 14, equivalent positions $\pm(x, y, z; {}^1/_2 - x, {}^1/_2 + y, {}^1/_2 - z)$). The asymmetric unit consists of half of the anion and one cation, the remainder being generated by an inversion center. Isotropic refinement converged at R = 10.9%. A difference map revealed a twofold disorder of the methylene carbon atoms of the cation.[24] The occupancies of these atoms refined to two sets of average values, 71% and 29%. These values were fixed during final anisotropic refinement on all non-hydrogen atoms.

(b) $(Et_4N)_2[Fe_2(X_2\text{-}o\text{-}xyl)_3]\cdot 2MeCN$. The systematic absences $h0l$ ($h + l = 2n + 1$) and $0k0$ ($k = 2n + 1$) uniquely define the space group $P2_1/n$. Isotropic refinement of all non-hydrogen atoms converged at R = 12%. Phenyl-ring carbon atoms were treated as rigid groups with isotropic thermal parameters, and all other non-hydrogen atoms were refined anisotropically.

(c) $(Et_4N)_2[Co_2(SEt)_6]$. This compound is isomorphous with $(Et_4N)_2[Fe_2(SEt)_6]$. The structure was solved by using the coordinates of $[Fe_2(SEt)_6]^{2-}$, and the remaining atoms were located from difference Fourier maps. Isotropic refinement converged at R = 9.9%. Further refinement indicated some cation disorder, with the minor orientation having an occupancy of 20%. All non-hydrogen atoms were refined anisotropically, and hydrogen atoms were included on all carbon atoms except those of the minority component of the disordered cation.

(d) $(n\text{-}Bu_4N)_2[Co_2(SEt)_6]$. The systematic absences $0kl$ ($k = 2n + 1$), $h0l$ ($l = 2n + 1$), and $hk0$ ($h = 2n + 1$) uniquely define the centrosymmetric space group $Pbca$. The asymmetric unit contains the entire anion and both cations. Large thermal parameters of several of the cation methyl carbon atoms indicated disorder in their positions, which was not successfully modeled. Isotropic refinement converged

---

[22] This procedure yielded orange-brown crystals and a few black crystals. The latter belong to a C-centered monoclinic space group with the unit cell dimensions a = 72.55 (6) Å, b = 14.074 (9) Å, c = 20.07 (1) Å, and β = 103.15 (5)°, derived from the transformation of a triclinic cell. The structure was not pursued owing to the long a axis. The unit cell volume (19950 Å^3) is slightly more than four times that of the orange-brown crystals whose structure is reported here.

[23] Cromer, D. T.; Waber, J. T. "International Tables for X-Ray Crystallography"; Kynoch Press: Birmingham, England, 1974.

[24] See paragraph at the end of this article regarding supplementary material available.

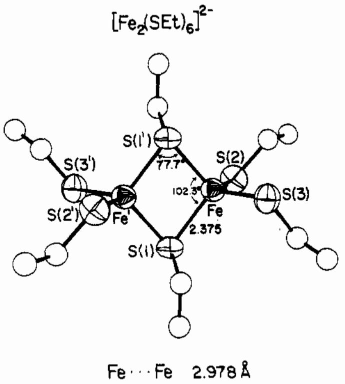

Figure 2. Structure of *anti*-$[Fe_2(SEt)_6]^{2-}$ as its Et_4N^+ salt. In this and subsequent figures, primed and unprimed atoms are related by an inversion center, and 50% probability ellipsoids, atom-labeling schemes, and selected distances and angles are presented. For clarity, carbon atoms are represented as spheres of arbitrary radius. An alternative view of the anti structure is provided in Figure 4.

Table II. Atom Coordinates of $[Fe_2(SEt)_6]^{2-}$ and $[Fe_2(S_2\text{-}o\text{-xyl})_3]^{2-}$

atom	x	y	z
	$[Fe_2(SEt)_6]^{2-}$		
Fe	0.0466 (1)[a]	0.0680 (1)	0.0745 (1)
S(1)	−0.1790 (1)	0.0451 (1)	−0.0145 (1)
S(2)	0.0228 (2)	0.0425 (1)	0.2244 (1)
S(3)	0.1404 (1)	0.2103 (1)	0.0570 (1)
C(11)[b]	−0.2060 (5)	0.1370 (4)	−0.1008 (4)
C(21)	−0.3463 (7)	0.1705 (6)	−0.1173 (6)
C(12)	0.1906 (7)	0.0667 (5)	0.2961 (4)
C(22)	0.1869 (13)	0.0708 (6)	0.3972 (5)
C(13)	0.0275 (12)	0.2874 (5)	0.1067 (7)
C(23)	0.0235 (11)	0.3734 (7)	0.0958 (8)
	$[Fe_2(S_2\text{-}o\text{-xyl})_3]^{2-}$		
Fe(1)	0.4264 (2)	0.1479 (1)	0.8175 (1)
Fe(2)	0.5674 (2)	0.1815 (1)	0.7008 (1)
S(1)	0.2773 (4)	0.0825 (2)	0.8239 (2)
S(2)	0.4843 (5)	0.1856 (2)	0.9312 (2)
S(3)	0.6142 (4)	0.1102 (2)	0.7859 (2)
S(4)	0.5578 (4)	0.1535 (2)	0.5827 (2)
S(5)	0.3662 (4)	0.2108 (2)	0.7232 (2)
S(6)	0.7238 (4)	0.2444 (2)	0.7372 (3)
C(1)S[c]	0.3826 (13)	0.0405 (6)	0.8917 (7)
C(2)S	0.5536 (14)	0.1247 (6)	0.9795 (8)
C(3)S	0.5547 (15)	0.0474 (6)	0.7395 (8)
C(4)S	0.5016 (14)	0.0832 (6)	0.5852 (8)
C(5)S	0.3765 (16)	0.2751 (6)	0.7679 (8)
C(6)S	0.6538 (17)	0.2992 (7)	0.7834 (10)
C(1)	0.3798 (8)	0.0540 (4)	0.9688 (5)
C(2)	0.2955 (8)	0.0247 (4)	1.0011 (5)
C(3)	0.2929 (8)	0.0329 (4)	1.0737 (5)
C(4)	0.3746 (8)	0.0705 (4)	1.1139 (5)
C(5)	0.4590 (8)	0.0999 (4)	1.0815 (5)
C(6)	0.4616 (8)	0.0916 (4)	1.0089 (5)
C(7)	0.6333 (10)	0.0305 (4)	0.6860 (4)
C(8)	0.7369 (10)	−0.0035 (4)	0.7115 (4)
C(9)	0.8119 (10)	−0.0223 (4)	0.6644 (4)
C(10)	0.7834 (10)	−0.0073 (4)	0.5919 (4)
C(11)	0.6799 (10)	0.0267 (4)	0.5665 (4)
C(12)	0.6048 (10)	0.0455 (4)	0.6135 (4)
C(13)	0.4218 (7)	0.3193 (4)	0.7272 (6)
C(14)	0.3328 (7)	0.3511 (4)	0.6814 (6)
C(15)	0.3751 (7)	0.3934 (4)	0.6443 (6)
C(16)	0.5065 (7)	0.4037 (4)	0.6531 (6)
C(17)	0.5955 (7)	0.3719 (4)	0.6990 (6)
C(18)	0.5532 (7)	0.3296 (4)	0.7360 (6)

[a] Numbers in parentheses in this and successive tables are the estimated standard deviations in the last figure(s). [b] S(n)–C(1n)–C(2n), n = 1–3. [c] Notation:

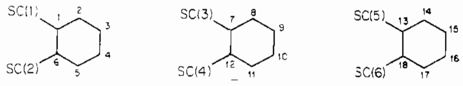

Table III. Atom Coordinates of *syn*- and *anti*-$[Co_2(SEt)_6]^{2-}$

atom	x	y	z
	syn-$[Co_2(SEt)_6]^{2-}$		
Co(1)	0.8661 (1)	0.2316 (1)	0.1134 (1)
Co(2)	0.9618 (1)	0.3302 (1)	0.1580 (1)
S(1)	0.9470 (2)	0.2194 (1)	0.1700 (1)
S(2)	0.8468 (2)	0.3430 (1)	0.1188 (1)
S(3)	0.9316 (2)	0.2088 (2)	0.0556 (1)
S(4)	0.7413 (2)	0.1914 (2)	0.1213 (1)
S(5)	0.9509 (2)	0.3739 (1)	0.2188 (1)
S(6)	1.0798 (2)	0.3484 (1)	0.1259 (1)
C(11)[a]	1.0387 (5)	0.1821 (4)	0.1542 (3)
C(21)	1.0473 (8)	0.1148 (5)	0.1697 (4)
C(12)	0.8815 (7)	0.3768 (5)	0.0725 (3)
C(22)	0.8374 (11)	0.4284 (7)	0.0605 (5)
C(13)	0.9260 (7)	0.1242 (7)	0.0553 (5)
C(23)	0.9879 (9)	0.0861 (7)	0.0482 (5)
C(14)	0.7499 (8)	0.1078 (5)	0.1350 (4)
C(24)	0.6906 (11)	0.0695 (7)	0.1338 (7)
C(15)	0.9169 (9)	0.4580 (5)	0.2117 (4)
C(25)	0.9316 (14)	0.5011 (9)	0.2386 (6)
C(16)	1.1077 (7)	0.4317 (6)	0.1391 (4)
C(26)	1.0677 (11)	0.4773 (8)	0.1191 (4)
	anti-$[Co_2(SEt)_6]^{2-}$		
Co	0.0485 (1)	0.0691 (1)	0.0769 (1)
S(1)	−0.1744 (1)	0.0420 (1)	−0.0109 (1)
S(2)	0.0215 (2)	0.0406 (1)	0.2237 (1)
S(3)	0.1465 (2)	0.2076 (1)	0.0581 (1)
C(11)[a]	−0.2080 (7)	0.1358 (5)	−0.0965 (5)
C(21)	−0.3428 (9)	0.1672 (6)	−0.1146 (7)
C(12)	0.1883 (8)	0.0689 (5)	0.2957 (4)
C(22)	0.1837 (12)	0.0694 (6)	0.3947 (5)
C(13)	0.0481 (15)	0.2860 (6)	0.1187 (9)
C(23)	0.0262 (12)	0.3685 (8)	0.1018 (8)

[a] S(n)–C(1n)–C(2n): n = 1–6 (syn), 1–3 (anti).

Table IV. Atom Coordinates of $[Fe_4(SEt)_{10}]^{2-}$

atom	x	y	z
Fe(1)	0.6813 (1)	0.1234 (1)	0.3815 (1)
Fe(2)	0.6612 (1)	0.1019 (1)	0.5595 (1)
Fe(3)	0.8440 (1)	0.1366 (1)	0.4903 (1)
Fe(4)	0.7619 (1)	−0.0047 (1)	0.4595 (1)
S(1)	0.6113 (1)	0.1417 (1)	0.4699 (1)
S(2)	0.7815 (1)	0.1752 (1)	0.4066 (1)
S(3)	0.6990 (1)	0.0305 (1)	0.3749 (1)
S(4)	0.7661 (2)	0.1512 (1)	0.5736 (1)
S(5)	0.6801 (1)	0.0102 (1)	0.5396 (1)
S(6)	0.8655 (1)	0.0434 (1)	0.4869 (1)
S(7)	0.6317 (2)	0.1517 (1)	0.2887 (1)
S(8)	0.5960 (2)	0.1149 (1)	0.6487 (1)
S(9)	0.9507 (1)	0.1800 (1)	0.5041 (2)
S(10)	0.7782 (2)	−0.0955 (1)	0.4494 (1)
C(11)[a]	0.5262 (7)	0.1081 (7)	0.4589 (6)
C(21)	0.5122 (10)	0.0644 (6)	0.4632 (8)
C(12)	0.8432 (6)	0.1750 (5)	0.3405 (5)
C(22)	0.8345 (9)	0.2104 (6)	0.2951 (7)
C(13)	0.7497 (8)	0.0219 (5)	0.3036 (5)
C(23)	0.7672 (12)	−0.0231 (7)	0.2866 (6)
C(14)	0.8096 (10)	0.1212 (7)	0.6417 (6)
C(24)	0.8298 (11)	0.1493 (8)	0.6818 (7)
C(15)	0.7176 (7)	−0.0176 (4)	0.6107 (4)
C(25)	0.6849 (8)	−0.0660 (5)	0.6303 (6)
C(16)	0.9385 (11)	0.0411 (8)	0.4247 (12)
C(26)	0.9550 (10)	−0.0026 (8)	0.4111 (10)
C(17)	0.5694 (8)	0.0983 (6)	0.2686 (6)
C(27)	0.4983 (8)	0.1141 (7)	0.2612 (8)
C(18)	0.5303 (8)	0.0623 (7)	0.6464 (7)
C(28)	0.4856 (10)	0.0570 (7)	0.6928 (8)
C(19)	0.9289 (7)	0.2505 (5)	0.5045 (6)
C(29)	0.8999 (7)	0.2714 (5)	0.5631 (7)
C(110)	0.6862 (8)	−0.1189 (5)	0.4418 (6)
C(210)	0.6687 (8)	−0.1481 (7)	0.3927 (7)

[a] S(n)–C(1n)–C(2n), n = 1–10.

at R = 11.1%. The structure was anisotropically refined on all non-hydrogen atoms.

Table V. Selected Interatomic Distances (Å) and Angles (deg) for *anti*-$[Fe_2(SEt)_6]^{2-}$ and *anti*-$[Fe_2(S_2\text{-}o\text{-xyl})_3]^{2-}$

anti-$[Fe_2(SEt)_6]^{2-}$		*anti*-$[Fe_2(S_2\text{-}o\text{-xyl})_3]^{2-}$	
$Fe-S_b$[a]			
Fe–S(1)	2.375 (1)	Fe(1)–S(3)	2.393 (5)
Fe–S(1′)	2.374 (1)	Fe(1)–S(5)	2.369 (5)
		Fe(2)–S(3)	2.387 (5)
		Fe(2)–S(5)	2.381 (5)
		mean	2.383 (10)
$Fe-S_t$[a]			
Fe–S(2)	2.304 (2)	Fe(1)–S(1)	2.300 (5)
Fe–S(3)	2.304 (2)	Fe(1)–S(2)	2.313 (5)
		Fe(2)–S(4)	2.324 (5)
		Fe(2)–S(6)	2.291 (5)
		mean	2.307 (14)
Fe···Fe			
Fe···Fe′	2.978 (1)	Fe(1)–Fe(2)	3.034 (4)
$S_b\cdots S_b$			
S(1)···S(1′)	3.699 (4)	S(3)···S(5)	3.662 (6)
S_b-Fe-S_b			
S(1)–Fe–S(1′)	102.3 (1)	S(3)–Fe(1)–S(5)	100.6 (2)
		S(3)–Fe(2)–S(5)	100.4 (2)
S_t-Fe-S_t			
S(2)–Fe–S(3)	111.7 (1)	S(1)–Fe(1)–S(2)	107.2 (2)
		S(4)–Fe(2)–S(6)	112.5 (2)
$Fe-S_b-Fe$			
Fe–S(1)–Fe′	77.7 (1)	Fe(1)–S(3)–Fe(2)	78.8 (2)
		Fe(1)–S(5)–Fe(2)	79.4 (1)
S_b-Fe-S_t			
S(1)–Fe–S(2)	104.9 (1)	S(3)–Fe(1)–S(1)	110.5 (2)
S(1)–Fe–S(3)	114.5 (1)	S(3)–Fe(1)–S(2)	108.6 (2)
		S(5)–Fe(1)–S(1)	115.6 (2)
		S(5)–Fe(1)–S(2)	114.1 (2)
		S(3)–Fe(2)–S(4)	112.7 (2)
		S(3)–Fe(2)–S(6)	105.9 (2)
		S(5)–Fe(2)–S(4)	113.7 (2)
		S(5)–Fe(2)–S(6)	110.8 (2)

[a] b = bridging ligand; t = terminal ligand.

Table VI. Selected Interatomic Distances (Å) and Angles (deg) for the Anti and Syn Forms of $[Co_2(SEt)_6]^{2-}$

anti-$[Co_2(SEt)_6]^{2-}$ [a]		*syn*-$[Co_2(SEt)_6]^{2-}$ [b]	
$Co-S_b$			
Co–S(1)	2.357 (2)	Co(1)–S(1)	2.358 (3)
Co–S(1′)	2.353 (2)	Co(1)–S(2)	2.369 (4)
		Co(2)–S(1)	2.375 (3)
		Co(2)–S(2)	2.349 (3)
		mean	2.363 (12)
$Co-S_t$			
Co–S(2)	2.274 (2)	Co(1)–S(3)	2.290 (4)
Co–S(3)	2.267 (2)	Co(1)–S(4)	2.262 (3)
		Co(2)–S(5)	2.261 (3)
		Co(2)–S(6)	2.279 (3)
		mean	2.273 (14)
Co···Co			
Co···Co′	3.045 (2)	Co(1)···Co(2)	3.020 (3)
$S_b\cdots S_b$			
S(1)···S(1′)	3.594 (4)	S(1)···S(2)	3.541 (6)
S_b-Co-S_b			
S(1)–Co–S(1′)	99.4 (1)	S(1)–Co(1)–S(2)	97.0 (1)
		S(1)–Co(2)–S(2)	97.1 (1)
S_t-Co-S_t			
S(2)–Co–S(3)	114.0 (1)	S(3)–Co(1)–S(4)	117.4 (1)
		S(5)–Co(2)–S(6)	115.8 (1)
$Co-S_b-Co$			
Co–S(1)–Co′	80.6 (1)	Co(1)–S(1)–Co(2)	79.3 (1)
		Co(1)–S(2)–Co(2)	79.6 (1)
S_b-Co-S_t			
S(1)–Co–S(2)	103.3 (1)	S(1)–Co(1)–S(3)	113.5 (1)
S(1)–Co–S(3)	116.9 (1)	S(1)–Co(1)–S(4)	112.9 (1)
		S(2)–Co(1)–S(3)	109.3 (1)
		S(2)–Co(1)–S(4)	103.6 (1)
		S(1)–Co(2)–S(5)	103.5 (1)
		S(1)–Co(2)–S(6)	109.6 (1)
		S(2)–Co(2)–S(5)	113.8 (1)
		S(2)–Co(2)–S(6)	114.5 (1)
		mean	110.1

[a] $n\text{-}Bu_4N^+$ salt. [b] Et_4N^+ salt.

(e) $(Me_4N)_2[Fe_4(SEt)_{10}]$. Systematic absences define the space group *Pbca*. The structure exhibited no disorder. Isotropic refinement converged at $R = 9.7\%$. Final refinement was carried out with anisotropic descriptions of all non-hydrogen atoms.

Other Physical Measurements. Absorption spectra were recorded with use of a Cary Model 14 or 219 spectrophotometer. ^1H NMR spectra were obtained with a Bruker WM-300 spectrometer operating at 300 MHz; chemical shifts downfield of Me_4Si internal standard are designated as negative. All measurements were made under anaerobic conditions and on freshly prepared solutions.

Results and Discussion

The role of thiolate ligands RS^- as bridges in main-group and, especially, transition-element compounds has been extensively documented by X-ray structural determinations. These ligands have been found in the μ_2-SR modes **5**–**7** and

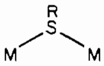

5

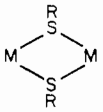

6

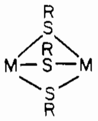

7

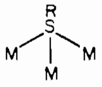

8

the μ_3-SR mode **8**. In complexes of iron and cobalt, the elements of interest here, examples of **5**,[25] **6**,[26–28] **7**,[29] and **8**[30] are known. The occurrence of the unsupported single bridge unit **5** is found with the adamantane-like cages such as **3** and the cyclic trimer **4**. Unit **7** has been established in several Fe(II) complexes, and unit **8** has been recognized only in a few trinuclear iron carbonyls. Far more pervasive is the unit **6**, which has been found in planar and nonplanar forms of widely differing dimensions in five- and six-coordinate complexes of Fe(I, II, III)[26,27a–c,28] and Co(II, III).[27d,28b] Here we describe the structures of the simplest complexes known to

---

(25) (a) $[M_4(SPh)_{10}]^{2-}$ (**3**): ref 11, 12, and 21. (b) $[Fe_4(\mu\text{-}SPh)_6Cl_4]^{2-}$: Coucouvanis, D.; Kanatzidis, M.; Simhon, E.; Baenziger, N. C. *J. Am. Chem. Soc.* **1982**, *104*, 1874. (c) $[M_3S(S_2\text{–}o\text{-xyl})_3]^{2-}$: ref 6. (d) $[Fe_3S(S_2\text{–}o\text{-xyl-4,5-}Me_2)_3]^{2-}$: ref 7. (e) $[Fe_3(SPh)_3Cl_6]^{3-}$: ref 3 and results to be published.

(26) (a) $Fe_2(\mu\text{-}SEt)_2(NO)_4$: Thomas, J. T.; Robertson, J. H.; Cox, E. G. *Acta Crystallogr.* **1958**, *11*, 599. (b) $Fe_2(\mu\text{-}SEt)_2(CO)_6$: Dahl, L. F.; Wei, C.-H. *Inorg. Chem.* **1963**, *2*, 328. (c) $(C_5H_5)_2Fe_2(\mu\text{-}SPh)_2(CO)_2$: Ferguson, G.; Hannaway, C.; Islam, K. M. S. *Chem. Commun.* **1968**, 1165. (d) $[(C_5H_5)_2Fe_2(\mu\text{-}SMe)_2(CO)_2]^+$: Connelly, N. G.; Dahl, L. F. *J. Am. Chem. Soc.* **1970**, *92*, 7472. (e) $[(C_5H_5)_2Fe_2(\mu\text{-}SR)_2L_2]^{0,+,2+}$: Terzis, A.; Rivest, R. *Inorg. Chem.* **1973**, *12*, 2132. Vergamini, P. J.; Kubas, G. J. *Prog. Inorg. Chem.* **1976**, *21*, 261.

(27) (a) $[Fe_2(SCH_2CH_2S)_4]^{2-}$: ref 17. (b) $Fe_2(\mu\text{-}SEt)_2(S_2CSEt)_4$: Coucouvanis, D.; Lippard, S. J.; Zubieta, J. *Ibid.* **1970**, *9*, 2775. (c) $[Fe_2(\mu\text{-}SEt)_2(CS_3)_2(S_2CSEt)_2]^{2-}$: Henkel, G.; Simon, W.; Strasdeit, H.; Krebs, B. *Inorg. Chim. Acta* **1983**, *70*, 29. (d) $Co_2(\mu\text{-}SEt)_2(S_2CSEt)_4$: Lewis, D. F.; Lippard, S. J.; Zubieta, J. *J. Am. Chem. Soc.* **1972**, *94*, 1563.

(28) (a) FeL, FeL′ ($SCH_2CH_2NMe(CH_2)_nNMeCH_2CH_2S$, $n = 2$ (L), $n = 3$ (L′)): Hu, W.; Lippard, S. J. *J. Am. Chem. Soc.* **1974**, *96*, 2366. (b) $[(ML)_2NO]^+$: Rabinowitz, H. N.; Karlin, K. D.; Lippard, S. J. *Ibid.* **1977**, *99*, 1420.

(29) (a) $[Fe_2(\mu\text{-}SMe)_3(CO)_6]^+$: Schultz, A. J.; Eisenberg, R. *Inorg. Chem.* **1973**, *12*, 518. (b) $[Fe_2(\mu\text{-}SH)_3(PhP(CH_2CH_2PPh_2)_2)_2]^+$: DiVaira, M.; Midollini, S.; Sacconi, L. *Ibid.* 1979, *18*, 3466.

(30) $HFe_3(CO)_9(SR)$, $[Fe_3(CO)_9(SR)]^-$: Bau, R.; Don, B.; Greatrex, R.; Haines, R. J.; Love, R. A.; Wilson, R. D. *Inorg. Chem.* **1975**, *14*, 3021. Winter, A.; Zsolnai, L.; Huttner, G. *Chem. Ber.* **1982**, *115*, 1286.

contain unit **6**, which are also the only binuclear homoleptic metal thiolates of proven structure. These complexes were prepared by reaction 2 (Figure 1) or by an analogous method in the case of Co(II) and are of composition $[M_2(SR)_6]^{2-}$. They contain planar and nonplanar and syn and anti versions of **6** with tetrahedral Fe(II) and Co(II) sites. Prior to this investigation the only $M^{II}{}_2S_6$ complexes of known structure were $Ni_2(S(CH_2CH_2S)_2)_2$[31] and $M_2(\mu\text{-}SR)_2(S_2CSR)_2$[32] (M = Ni(II), Pd(II)), which contain nonplanar units **6**.

Structures of $[M_2(SR)_6]^{2-}$ Complexes. The structures of four compounds containing binuclear anions were determined (Table I). All crystal structures contained well-separated cations and anions. Other than displaying certain aspects of disorder, cation structures are unexceptional.[24] Selected interatomic distances and angles of the Fe(II) and Co(II) structures are collected in Tables V and VI, respectively.

(a) $[Fe_2(SEt)_6]^{2-}$ and $[Fe_2(S_2\text{-}o\text{-}xyl)_3]^{2-}$. The structure of $[Fe_2(SEt)_6]^{2-}$ as its Et_4N^+ salt is presented in Figure 2. The anion is formed by two $Fe(SEt)_3$ units sharing a tetrahedral edge. Because the anion has crystallographically imposed centrosymmetry, the $Fe_2(\mu\text{-}S)_2$ unit is planar with the anti configuration **2**. The bridge (b) angle at sulfur, Fe–S(1)–Fe′ = 77.7 (1)°, is somewhat larger than the value of 70.5° for an edge-shared perfect tetrahedral dimer.[33] Consequently, the angle S(1)–Fe–S(1′) = 102.3 (1)° is less than 109.5°. The Fe_2S_6 portion, of actual C_i symmetry, closely approaches an idealized D_{2h} arrangement. The two independent Fe–S_b distances (2.374 (1), 2.375 (1) Å) are indistinguishable as are the terminal (t) ligand distances Fe–S_t (both at 2.304 (2) Å). The bridge unit takes the form of a rhombus in which the nonbonding $S_b \cdots S_b'$ distance of 3.699 (4) Å is ~0.7 Å longer than the Fe···Fe′ separation of 2.978 (1) Å. These units in the other binuclear complexes, considered below, have a similar shape. The only significant departures from D_{2h} symmetry are found in the two independent S_b–Fe–S_t angles, which differ by 9.6°. This has the effect of placing pairs of S_t atoms at unequal distances above and below the $Fe_2(\mu\text{-}S)_2$ plane.[24]

A species corresponding to the composition $[Fe_2(S_2\text{-}o\text{-}xyl)_3]^{2-}$ was prepared by the reaction of $[FeCl_4]^{2-}$ with 2 equiv of $(S_2\text{-}o\text{-}xyl)^{2-}$ in ethanol.[13] In this solvent it exists in equilibrium 5 with the reduced rubredoxin site analogue $[Fe(S_2\text{-}o\text{-}xyl)_2]^{2-}$.[14]

$$[Fe_2(S_2\text{-}o\text{-}xyl)_3]^{2-} + (S_2\text{-}o\text{-}xyl)^{2-} \rightleftharpoons 2[Fe(S_2\text{-}o\text{-}xyl)_2]^{2-} \quad (5)$$

The binuclear complex has three potential isomeric forms with anti (**9**) and syn (**10, 11**) bridging units.

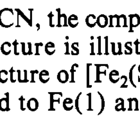

9

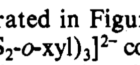

10

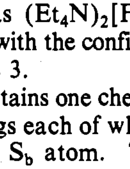

11

Forms **9** and **10** were originally recognized,[14] but at the time it was uncertain if the chelate ligand would span coordination positions on two Fe(II) atoms in the necessarily syn form **11**. When crystallized from acetonitrile as $(Et_4N)_2[Fe_2(S_2\text{-}o\text{-}xyl)_3]\cdot 2MeCN$, the complex is binuclear with the configuration **9**. Its structure is illustrated in Figure 3.

The structure of $[Fe_2(S_2\text{-}o\text{-}xyl)_3]^{2-}$ contains one chelate ring coordinated to Fe(1) and two other rings each of which furnishes one S_t atom to Fe(2) and one S_b atom. This arrangement necessitates an anti arrangement of bridging thiolate groups. As in tetrahedral $[Fe(S_2\text{-}o\text{-}xyl)_2]^{2-,-}$,[14] the rings adopt a chairlike conformation. The S(1)···S(2) bite distance of 3.713 (6) Å in the terminal seven-membered ring is decidedly smaller than the mean value (3.89 Å) in $[Fe(S_2\text{-}o\text{-}xyl)_2]^{2-}$.[14] The anion as a whole has no symmetry, and its Fe_2S_6 portion departs appreciably from idealized D_{2h} and even C_2 symmetry. The Fe–S_b and Fe–S_t distances fall in the ranges 2.369 (5)–2.393 (5) and 2.291 (5)–2.324 (5) Å, respectively. Further, the $Fe_2(\mu\text{-}S)_2$ unit is nonplanar with Fe(1, 2) and S(3, 5) atom displacements, on opposite sides of the least-squares plane, being 0.055 and 0.090 Å, respectively. Substantial variations in $S_{b,t}$–Fe–S_t bond angles reflect deviations from either idealized symmetry, as do inequalities in the associated $S_b \cdots S_t$ nonbonded distances S(3)···S(4) (3.922 (6) Å) and S(5)···S(6) (3.846 (7) Å) of the other two rings.

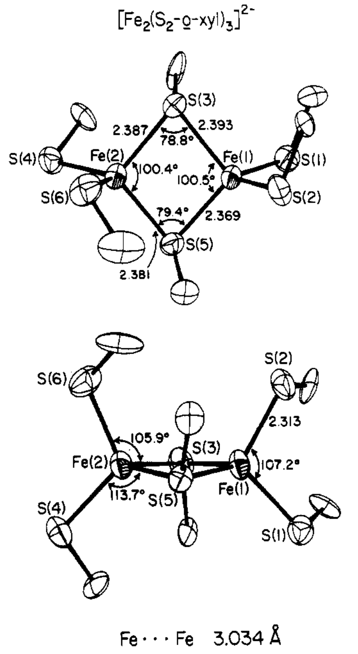

Figure 3. Two views of the structure of $[Fe_2(S_2\text{-}o\text{-}xyl)_3]^{2-}$ as its Et_4N^+ salt in bis(acetonitrile) solvate. The atom pairs S(1)–S(2), S(3)–S(4), and S(5)–S(6) belong to the same chelate ring.

Subsequent to our initial report of $[Fe_2(SEt)_6]^{2-}$,[3] Henkel et al.[34] reported the syntheses and structures of $(Me_4N)_2[Fe_2(S_2\text{-}o\text{-}xyl)_2(SPh)_2]\cdot{}^1/_3MeCN\cdot{}^2/_3THF$ and $(Me_4N)_2[Fe_2(S_2\text{-}o\text{-}xyl)_3]\cdot 5MeOH$. In the anion of the former compound each chelate ligand supplies one S_t and one S_b atom to a bridge unit in the anti form. The benzenethiolate ligands occupy terminal positions. In the latter compound the anion has the syn structure **11** in which one ligand occupies terminal, cisoid positions separated by ~4.3 Å. The structural flexibility of the ligand is well illustrated in this series of complexes where it closes 7- and 9-membered rings with S···S distances in the range 3.7–4.3 Å. In all but the 9-membered ring associated with structure **11**, the ligand adopts the chairlike conformation evident in Figure 3. Given that $S_b \cdots S_b$ distances are ~3.7 Å, this conformation would presumably destabilize the experimentally unrealized structure **10** by virtue of unfavorable interactions of the bridging ligand with a S_t atom of one of the terminal chelate rings. The only other complex of the $[Fe_2(SR)_6]^{2-}$ type is $[Fe_2(SCH_2CH_2(S)CH_2OH)_4]^{2-}$, which has been identified in aqueous solution[35] but not isolated.

(b) *anti*- and *syn*-$[Co_2(SEt)_6]^{2-}$. $(Et_4N)_2[Co_2(SEt)_6]$ is isomorphous with its Fe(II) analogue. As shown in Figure 4, $[Co_2(SEt)_6]^{2-}$ also has the centrosymmetric anti structure;

---

(31) Baker, D. J.; Goodall, D. C.; Moss, D. S. *Chem. Commun.* **1969**, 325. Barclay, G. A.; McPartlin, E. M.; Stephenson, N. C. *Acta Crystallogr., Sect. B* **1969**, *B25*, 1262.

(32) Chiesa Villa, A.; Manfredotti, A. G.; Nardelli, M.; Pellizzi, C. *Chem. Commun.* **1970**, 1322. Fackler, J. P., Jr.; Zegarski, W. J. *J. Am. Chem. Soc.* **1973**, *95*, 8566.

(33) Summerville, R. H.; Hoffmann, R. *J. Am. Chem. Soc.* **1976**, *98*, 7240.

(34) Henkel, G.; Tremel, W.; Krebs, B. *Angew. Chem., Int. Ed. Engl.* **1983**, *22*, 319; *Angew. Chem. Suppl.* **1983**, 323.

(35) Leussing, D. L.; Jayne, J. *J. Phys. Chem.* **1962**, *66*, 426.

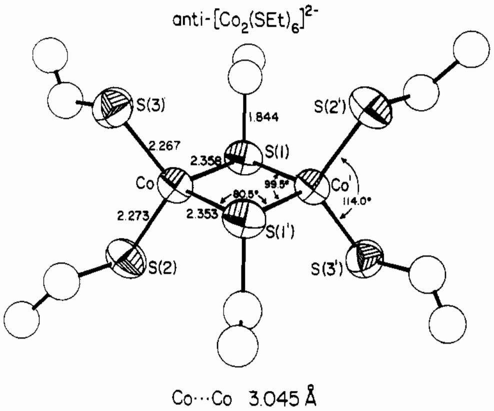

Figure 4. Structure of *anti*-$[Co_2(SEt)_6]^{2-}$ as its Et_4N^+ salt.

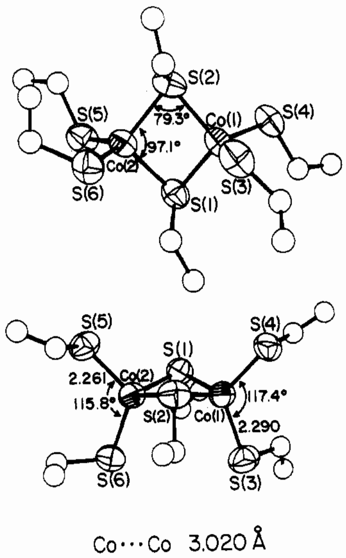

Figure 5. Two views of the structure of *syn*-$[Co_2(SEt)_6]^{2-}$ as its *n*-Bu_4N^+ salt.

consequently, all structural features of it and $[Fe_2(SEt)_6]^{2-}$ are quite comparable. The uniformly shorter Co–S distances are expected from the smaller tetrahedral radius of Co(II) (0.72 Å) compared to Fe(II) (0.77 Å).[36] When crystallized in the form of its *n*-Bu_4N^+ salt, $[Co_2(SEt)_6]^{2-}$ is stabilized in the syn arrangement **2** illustrated in Figure 1 for the as yet unknown form of $[Fe_2(SEt)_6]^{2-}$. Although there is no imposed symmetry, inspection of the structure in Figure 5 and the metric data in Table VI reveals that the entire anion approaches C_2 symmetry. The $Co_2(\mu\text{-}S)_2$ bridge unit is decidedly nonplanar with Co(II) and S_b atoms on opposite sides of the weighted least-squares plane. The dihedral angle of this plane and that for the $Co_2(S_t)_4$ atom set is 90.1°, in close agreement with C_{2v} symmetry. However, the division of Co–S_b distances into the pairs Co(1)–S(1) = 2.358 (3) Å, Co(2)–S(2) = 2.349 (3) Å and Co(1)–S(2) = 2.369 (4) Å, Co(2)–S(1) = 2.375 (3) Å indicates that C_2 is the more appropriate symmetry description of the bridge unit. Binuclear tetrahedral species of the type $[Co_2(SR)_6]^{2-}$ were anticipated (but not isolated) by Dance[21b] in his consideration of the equilibria of Co^{II}/PhS^- solutions in acetonitrile.

(c) Summary. The following are the principal structural and related features of four binuclear complexes.

(i) The species $[M_2(SR)_6]^{2-}$ are formed by two edge-shared, imperfect tetrahedra that form a planar or nonplanar, *syn*- or *anti*-$[M_2(\mu\text{-}SR)_2]$ bridge unit **6** with the angles M–S_b–M and S_b–M–S_b larger and smaller, respectively, than those of a perfect tetrahedral dimer. The separation $S_b \cdots S_b$ exceeds M···M by 0.5–0.7 Å. The (distorted) tetrahedral coordination of Fe(II) and Co(II) is found without exception in homoleptic thiolate complexes of these ions[9–12,14,21,34] and is otherwise consistent with their stereochemical tendencies in structurally unconstrained molecules.[37] The binuclear tetrahedral structure extends to $[M_2(SR)_6]^{2-}$, with M = Mn(II), Zn(II) and Cd(II),[38] ions with a tetrahedral stereochemical preference when four-coordinate.

(ii) The planar anti bridge arrangement occurs in Et_4N^+ salts of $[M_2(SEt)_6]^{2-}$, with M = Mn(II), Fe(II), Co(II), Zn(II), and Cd(II), and the nonplanar syn form occurs in the *n*-Bu_4N^+ salt of $[Co_2(SEt)_6]^{2-}$. Because the syn ⇄ anti interconversion is not frozen out in low-temperature ^1H NMR spectra (vide infra), the interconversion is facile and the isolation of a given form is presumably dependent on crystal packing energetics. Although *syn*-$[Co_2(SEt)_6]^{2-}$ and *syn*-$[Fe_2(S_2\text{-}o\text{-}xyl)_3]^{2-}$[34] (**11**) have nonplanar bridge units, insufficient examples exist to correlate these two structural features.

(iii) The usual order of bond distances to bridging and terminal ligands, here M–S_b > M–S_t, prevails. In terms of mean distances, the difference is 0.07–0.08 Å for Fe(II) and 0.08–0.09 Å for Co(II). Mean M–S_t distances in *anti*-$[Fe_2(SEt)_6]^{2-}$, *syn*-[34] and *anti*-$[Fe_2(S_2\text{-}o\text{-}xyl)_3]^{2-}$, $[Fe_4(SEt)_{10}]^{2-}$ (vide infra), and $[Fe_4(SPh)_{10}]^{2-}$[12] differ by <0.01 Å. The same is true for *syn*- and *anti*-$[Co_2(SEt)_6]^{2-}$ and $[Co_4(SPh)_{10}]^{2-}$.[21] In contrast the bond distances in $[Fe(SPh)_4]^{2-}$,[10] $[Fe(S_2\text{-}o\text{-}xyl)_2]^{2-}$,[14] and $[Co(SPh)_4]^{2-}$[9] in the respective comparisons are ~0.05 Å longer. This is a rather clear illustration of the effect of bridging ligands on metal–terminal ligand bond distances; viz., the decreased charge donor capacity of the bridging ligand to each metal induces a compensation in terms of shortened terminal ligand bond lengths at the metal sites.

Structural comparisons of the present set of complexes with those of iron or cobalt containing the bridge unit **6**[26–28] are not profitable owing to differences in coordination number and/or metal oxidation state. Of these, only $Fe_2(SEt)_2(NO)_4$[26a] is an edge-shared tetrahedral dimer, but its bridge dimensions and diamagnetic electronic structure are very different from those of the $[M_2(SR)_6]^{2-}$ set examined here. The Fe(II) complexes of types **2**–**4** are antiferromagnetic.[39] The electronic structures of $[Fe_2(SR)_6]^{2-}$ complexes will be dealt with in a subsequent report describing magnetic properties. Summerville and Hoffmann[33] have presented an extended Hückel treatment of other examples of tetrahedral dimers.

Solution Equilibria of $[M_2(SR)_6]^{2-}$ Complexes. UV–visible absorption spectra of solutions of salts of $[Co(SEt)_4]^{2-}$, $[Co_2(SEt)_6]^{2-}$, and $[Co_4(SEt)_{10}]^{2-}$ in acetonitrile are given in Figure 6. Spectra in the LMCT (<500 nm) and ligand field regions are typical of tetrahedral $Co^{II}(SR)_4$ chromophores.[8,14,21] The features at 600–750 nm are components of the ν_3 ($^4A_2 \rightarrow {}^4T_1(P)$) transition in tetrahedral symmetry. The ν_2 bands ($^4A_2 \rightarrow {}^4T_1(F)$, not shown) appear at λ_{max} 1230–1320 nm. Tetrahedral $Fe^{II}(SR)_4$ chromophores exhibit the $^5E \rightarrow {}^5T_2$ band as a broad feature at λ_{max} 1700–2000 nm.[2,4,10,14] Absorption spectra of the mono-, bi-, and tetranuclear Fe(II) and Co(II) complexes are consistent with retention of tetrahedral coordination in solution but do not otherwise identify the structures of the solute species. This matter is more effectively pursued by ^1H NMR inasmuch as the large isotropic shifts induced by tetrahedral Fe(II) and Co(II) tend to afford fully resolved spectra.[2,4,6,12]

---

[36] Shannon, R. D. *Acta Crystallogr., Sect. A* **1976**, *A32*, 751.

[37] Holm, R. H.; O'Connor, M. J. *Prog. Inorg. Chem.* **1971**, *14*, 241.

[38] Watson, A. D.; Holm, R. H., results to be submitted for publication.

[39] Girerd, J.-J.; Gamp, E.; Hagen, K. S.; Edelstein, N.; Holm, R. H., results to be submitted for publication.

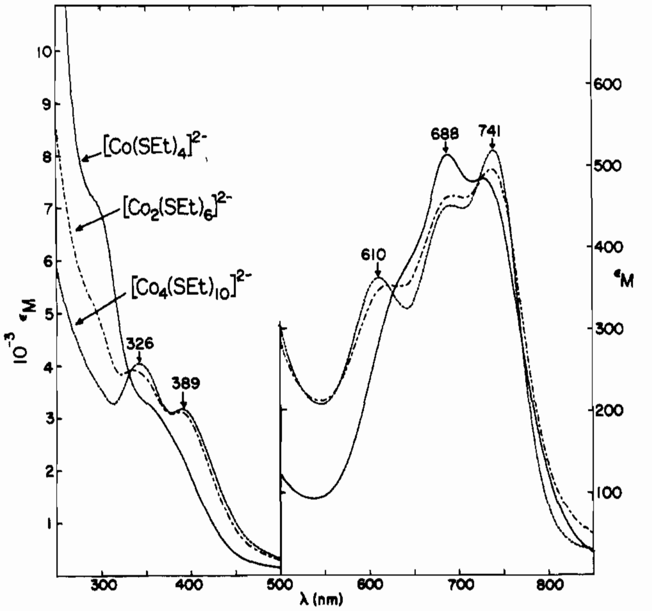

Figure 6. Absorption spectra of $[Co(SEt)_4]^{2-}$, $[Co_4(SEt)_{10}]^{2-}$, and a solution prepared from $(Et_4N)_2[Co_2(SEt)_6]$ in acetonitrile. Nominal solute concentrations are 1–2 mM.

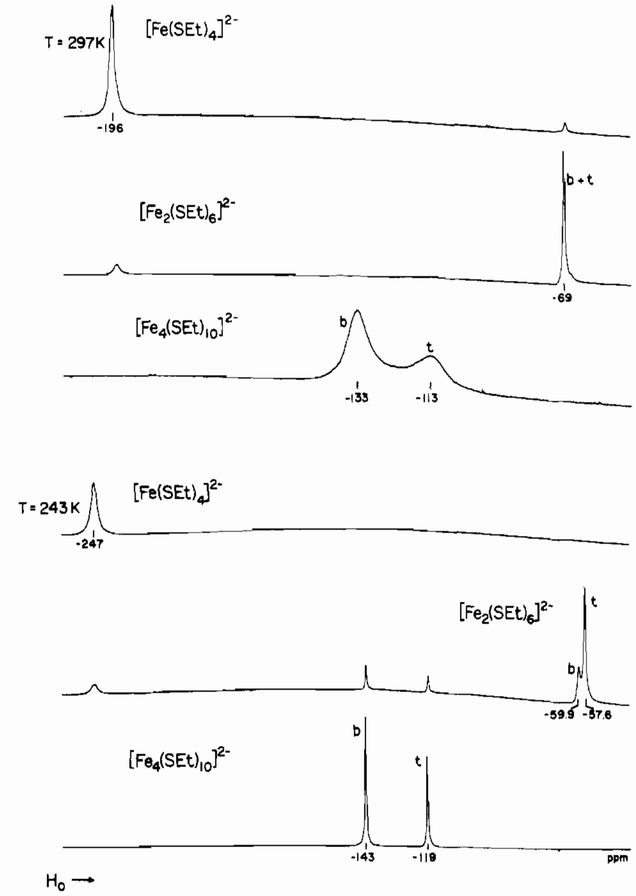

Figure 7. ^1H NMR spectra of $[Fe(SEt)_4]^{2-}$, $[Fe_2(SEt)_6]^{2-}$, and $[Fe_4(SEt)_{10}]^{2-}$ in CD_3CN solutions (~20 mM) at 297 K (upper) and 243 K (lower). In this and the following figure, CH_2 resonances of bridging (b) and terminal (t) ligands are shown; CH_3 resonances occur at higher field.

^1H NMR spectra of $[Fe(SEt)_4]^{2-}$, $[Fe_2(SEt)_6]^{2-}$, and $[Fe_4(SEt)_{10}]^{2-}$ at 297 and 243 K in CD_3CN solutions are shown in Figure 7; only CH_2 resonances, all of which occur in the more downfield regions of the spectra, are included. The solution prepared from $(Et_4N)_2[Fe_2(SEt)_6]$ gives a spectrum at 297 K consisting of a resonance at −69 ppm, assigned to bridging and terminal ligands of $[Fe_2(SEt)_6]^{2-}$, a weak monomer peak at −196 ppm, and two very broad and weak features just discernible at about −110 and −130 ppm. At the lower temperature, resolution is improved. Terminal and bridging resonances of the dimer are evident, the monomer peak is retained, and the terminal and bridging signals assigned to $[Fe_4(SEt)_{10}]^{2-}$ are sharp and well resolved. Spectra of the analogous set of Co(II) complexes at the same temperatures are presented in Figure 8. Spectra of solutions prepared from $(Et_4N)_2[Co_2(SEt)_6]$ exhibit at both temperatures resonances of $[Co(SEt)_4]^{2-}$ and $[Co_4(SEt)_{10}]^{2-}$ as well as those assigned to the dimer, which have a 2:1 t:b intensity ratio. Addition of $[Co(SEt)_4]^{2-}$ to a solution containing $[Co_2(SEt)_6]^{2-}$ increases the signal intensities of the latter relative to those of $[Co_4(SEt)_{10}]^{2-}$ (spectrum B, Figure 8). The only isotropically shifted resonances observed are those attributable to three species in the Fe(II) and Co(II) systems. These findings are consistent with the existence of equilibrium 6. Further, Et_4N^+

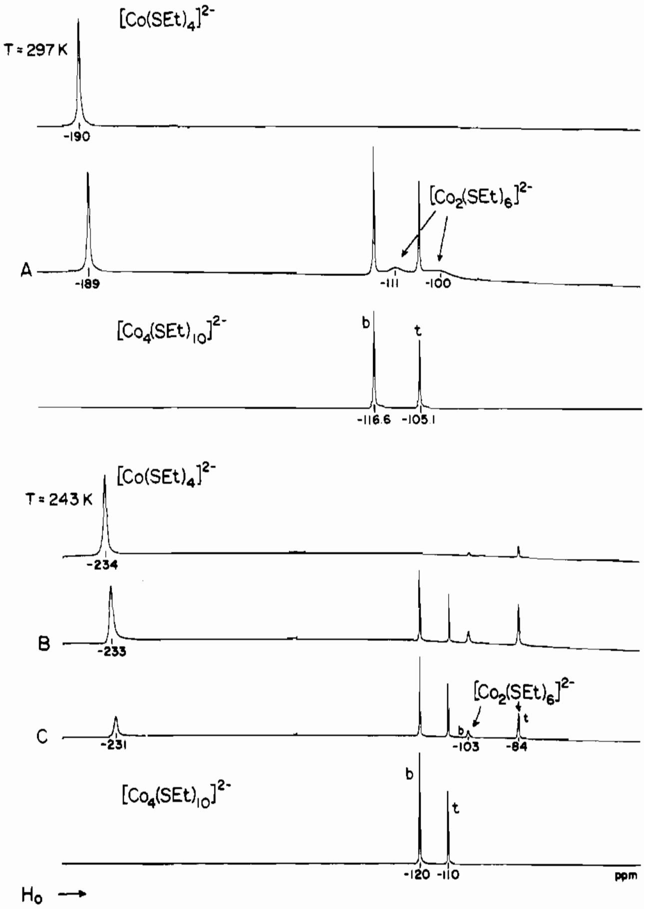

Figure 8. ^1H NMR spectra of $[Co(SEt)_4]^{2-}$, $[Co_2(SEt)_6]^{2-}$, and $[Co_4(SEt)_{10}]^{2-}$ in CD_3CN solutions at 297 K (upper) and 243 K (lower). Spectra A–C are those of solutions prepared from $(Et_4N)_2[Co_2(SEt)_6]$ with a nominal dimer concentration of 50 mM. Spectrum B is that of a solution to which $[Co(SEt)_4]^{2-}$ was added, giving a nominal monomer:dimer mole ratio of 1:1.

$$3[M_2(SEt)_6]^{2-} \rightleftharpoons 2[M(SEt)_4]^{2-} + [M_4(SEt)_{10}]^{2-} \quad (6)$$

salts of both $[Co_2(SEt)_6]^{2-}$ and $[Co_4(SEt)_{10}]^{2-}$ were isolated from a 3:1 NaSEt:$CoCl_2$ reaction system in acetonitrile. Although equilibrium constants have not been accurately determined, it is evident that $K_{Co} >> K_{Fe}$. As seen in Figure 6, the absorption spectrum of a solution prepared from $(Et_4N)_2[Co_2(SEt)_6]$ contains features corresponding to those of $[Co(SEt)_4]^{2-}$ and $[Co_4(SEt)_{10}]^{2-}$.

Several features of the NMR spectra require further comment. In CD_3CN solutions at ~240 K, *syn*- and *anti*-[Co₂-

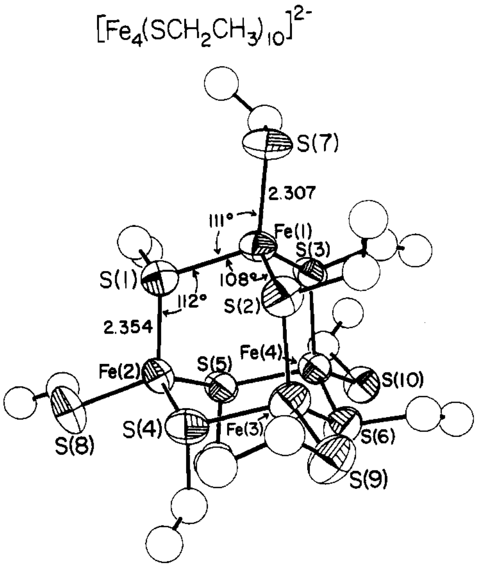

Figure 9. Structure of $[Fe_4(SEt)_{10}]^{2-}$ as its Me_4N^+ salt. Selected mean bond distances and angles are given.

$(SEt)_6]^{2-}$ give identical spectra. At temperatures as low as 200 K in acetone-d_6 solutions, no splittings of the resonances of $[M_2(SEt)_6]^{2-}$ into those of syn and anti forms have been observed. Coalescence of the two resonances of $[Fe_2(SEt)_6]^{2-}$ at 243 K to a single feature at 297 K and a broadening (without coalescence) of the two resonances of $[Co_2(SEt)_6]^{2-}$ over this temperature interval are indicative of an exchange process. Analogous behavior has been observed for $[Fe_4(SPh)_{10}]^{2-}$ and $[Co_4(SPh)_{10}]^{2-}$ and has been shown to arise from intramolecular b ⇄ t ligand interchange.[12] A similar process is probable here, and the proposed mechanism for ligand equilibration[12] is applicable to the dimers. The broadened spectrum of $[Fe_4(SEt)_{10}]^{2-}$ at 297 K (Figure 7) is similarly interpreted. This behavior and the 3:2 b:t signal intensity ratio in the low-temperature Fe(II) and Co(II) spectra support formulation of the two $[M_4(SEt)_{10}]^{2-}$ complexes in terms of the adamantane-like structure **3**. However, all previous *proven* examples of transition-element compounds with this structure (vide infra) contain arenethiolate (PhS^-) rather than alkylthiolate ligands. Consequently, the spectral assignments leading to reaction 6 required a demonstrated structure for $[M_4(SEt)_{10}]^{2-}$. This matter was addressed in the form of an X-ray structure determination of $(Me_4N)_2[Fe_4(SEt)_{10}]$.

Structure of $[Fe_4(SEt)_{10}]^{2-}$. Selected interatomic distance and angle data are compiled in Table VII. The structure, presented in Figure 9, immediately reveals that $[Fe_4(SEt)_{10}]^{2-}$ does possess the structure **3** with an adamantane-like $Fe_4(\mu\text{-}S)_6$ cage. This substantiates NMR signal assignments in the Fe(II) system and, by obvious analogy, those in the Co(II) system and therewith the existence of equilibrium 6. The complex is structurally closely related to the discrete cage species $[M_4(SPh)_{10}]^{2-}$ (M = Mn(II),[40] Fe(II),[11,12] Co(II),[21] Zn(II),[41] Cd(II)[42]), $[Fe_4(SPh)_6Cl_4]^{2-}$,[25b] and $[Zn_4(SPh)_8Cl_2]^{2-}$.[43] Because the structures of all but $[Zn_4(SPh)_{10}]^{2-}$ have been reported and described in considerable detail and a comparison of structures is available elsewhere,[40] no detailed account of the stereochemistry of $[Fe_4(SEt)_{10}]^{2-}$ is required here. When averaged under idealized T_d symmetry, all bonding and nonbonding (Fe···Fe, S_b···S_b) distances and angles of bonded atoms of the Fe_4S_{10} portions of $[Fe_4(SEt)_{10}]^{2-}$ and $[Fe_4(SPh)_{10}]^{2-}$ agree to ≤0.05 Å and <1°, respectively. In terms of axial ethyl or phenyl groups in the four chair Fe_3S_3 rings of the cages, $[Fe_4(SEt)_{10}]^{2-}$, as $[Fe_4(SPh)_{10}]^{2-}$, has the 3–2–1–0 pattern. These arrangements are described in terms of the number of axial substituents in each ring and are the counterparts of syn–anti isomerism in $[M_2(SR)_6]^{2-}$ complexes.

Table VII. Selected Interatomic Distances (Å) and Angles (deg) for $[Fe_4(SEt)_{10}]^{2-}$

	$Fe\text{-}S_t$[a]		
Fe(1)-S(7)	2.321 (3)	Fe(4)-S(10)	2.295 (3)
Fe(2)-S(8)	2.308 (4)	mean	2.307 (11)
Fe(3)-S(8)	2.303 (4)		
	$Fe\text{-}S_b$[a]		
Fe(1)-S(1)	2.362 (3)	Fe(3)-S(4)	2.349 (3)
Fe(1)-S(2)	2.350 (3)	Fe(3)-S(6)	2.358 (4)
Fe(1)-S(3)	2.343 (3)	Fe(4)-S(3)	2.347 (3)
Fe(2)-S(1)	2.369 (3)	Fe(4)-S(5)	2.346 (3)
Fe(2)-S(4)	2.347 (3)	Fe(4)-S(6)	2.366 (3)
Fe(2)-S(5)	2.352 (3)	mean	2.354 (9)
Fe(3)-S(2)	2.362 (4)		
	S-C		
range	1.80 (1)– 1.92 (2)	mean	1.84 (3)
	Fe···Fe		
Fe(1)···Fe(2)	3.898 (3)	Fe(2)···Fe(4)	3.913 (3)
Fe(1)···Fe(3)	3.876 (3)	Fe(3)···Fe(4)	3.902 (3)
Fe(1)···Fe(4)	3.915 (3)	mean	3.89 (2)
Fe(2)···Fe(3)	3.852 (3)		
	S_b···S_b		
S(1)···S(2)	3.583 (4)	S(3)···S(5)	3.609 (4)
S(1)···S(3)	3.822 (4)	S(3)···S(6)	3.975 (5)
S(1)···S(4)	3.685 (5)	S(4)···S(5)	3.939 (5)
S(1)···S(5)	3.832 (4)	S(4)···S(6)	3.771 (5)
S(2)···S(3)	3.984 (5)	S(5)···S(6)	3.766 (5)
S(2)···S(4)	3.666 (5)	mean	3.81 (15)
S(2)···S(6)	4.037 (5)		
	$S_b\text{-}Fe\text{-}S_t$		
S(1)-Fe(1)-S(7)	114.5 (1)	S(4)-Fe(3)-S(9)	111.9 (1)
S(2)-Fe(1)-S(7)	110.8 (1)	S(6)-Fe(3)-S(9)	108.5 (1)
S(3)-Fe(1)-S(7)	107.7 (1)	S(3)-Fe(4)-S(10)	111.3 (1)
S(1)-Fe(2)-S(8)	114.3 (1)	S(5)-Fe(4)-S(10)	108.2 (1)
S(4)-Fe(2)-S(8)	105.5 (1)	S(6)-Fe(4)-S(10)	114.4 (1)
S(5)-Fe(2)-S(8)	111.7 (1)	mean	110.7
S(2)-Fe(3)-S(9)	110.1 (1)		
	$S_b\text{-}Fe\text{-}S_b$		
S(1)-Fe(1)-S(2)	99.0 (1)	S(2)-Fe(3)-S(6)	117.6 (1)
S(1)-Fe(1)-S(3)	108.6 (1)	S(4)-Fe(3)-S(6)	106.5 (1)
S(2)-Fe(1)-S(3)	116.2 (1)	S(3)-Fe(4)-S(5)	100.5 (1)
S(1)-Fe(2)-S(4)	102.8 (1)	S(3)-Fe(4)-S(6)	115.0 (1)
S(1)-Fe(2)-S(5)	108.5 (1)	S(5)-Fe(4)-S(6)	106.1 (1)
S(4)-Fe(2)-S(5)	113.9 (1)	mean	108.1
S(2)-Fe(3)-S(4)	102.2 (1)		
	$Fe\text{-}S_b\text{-}Fe$		
Fe(1)-S(1)-Fe(2)	110.9 (1)	Fe(2)-S(5)-Fe(4)	112.8 (1)
Fe(1)-S(2)-Fe(3)	110.7 (1)	Fe(3)-S(6)-Fe(4)	111.4 (1)
Fe(1)-S(3)-Fe(4)	113.2 (1)	mean	111.5
Fe(2)-S(4)-Fe(3)	110.2 (1)		

[a] t = terminal ligand; b = bridging ligand.

The research described here is part of a series of investigations of Fe(II)–thiolate complexes that has included synthesis and structural, electronic, and reactivity characterization of $[Fe(SR)_4]^{2-}$ (**1**),[2-4,14] $[Fe_2(SR)_6]^{2-}$ (**2**),[3,13,14] and $[Fe_4(SR)_{10}]^{2-}$.[2,11,12] Other groups have provided significant contributions to the chemistry of the complexes **1**[8,10] and **2**.[34] Because no complexes with a nuclearity greater than four or, in the case of smaller nuclearities, with structures different from **1**–**3** have been found, the remaining area of investigation centers on the trinuclear cyclic anions $[Fe_3(SR)_3X_6]^{3-}$ (**4**). The remarkable nature of the essentially planar ring of $[Fe_3$-

---

(40) Costa, T.; Dorfman, J. R.; Hagen, K. S.; Holm, R. H. *Inorg. Chem.* **1983**, *22*, 4091.

(41) Hencher, J. L.; Khan, M.; Said, F. F.; Tuck, D. G. *Inorg. Nucl. Chem. Lett.* **1981**, *17*, 287.

(42) Hagen, K. S.; Holm, R. H. *Inorg. Chem.* **1983**, *22*, 3170.

(43) Dance, I. G. *Inorg. Chem.* **1981**, *20*, 2155.

$(SPh)_3Cl_6]^{3-}$ [3] is underscored by the large and thus strained Fe–S_b–Fe angles (139, 142°) compared to those of $[Fe_2(SR)_6]^{2-}$ (78–79°) and $[Fe_4(SR)_{10}]^{2-}$ (94–118°). This species undergoes structural changes in solution that, together with solid-state structural and other aspects of type **4** complexes, will be the subject of a future paper.

Acknowledgment. This research was supported by NIH Grant GM 28856. NMR and X-ray diffraction equipment used in this research was obtained by NSF Grants CHE 80-00670 and CHE 80-08891.

Registry No. *anti*-**2** (R = Et), 88294-16-0; **3** (R = Et), 88271-63-0; **9**, 88271-72-1; $(Me_4N)_2[Co(SEt)_4]$, 88271-65-2; $(Et_4N)_2[Co_4(SEt)_{10}]$, 88271-67-4; $(Et_4N)_2[Co_2(SEt)_6]$, 88271-69-6; $(n\text{-}Bu_4N)_2[Co_2(SEt)_6]$, 88294-18-2.

Supplementary Material Available: Listings of cation and solvate atom coordinates, temperature factors of cations, anions, and solvate molecules, hydrogen atom coordinates and isotropic temperature factors, atom deviations from $Fe_2(\mu\text{-}S)_2$ least-squares planes, and observed and calculated structure factors and a stereoview of $[Fe_2(S_2\text{-}o\text{-}xyl)_3]^{2-}$ (90 pages). Ordering information is given on any current masthead page.

Contribution from the Lehrstuhl für Anorganische Chemie I der Ruhr-Universität, D-4630 Bochum, West Germany,
and the Max-Planck-Institut für Kohlenforschung, D-4330 Mülheim a.d. Ruhr, West Germany

Reactions of $LM(CO)_3$ Complexes (M = Cr, Mo, W; L = 1,4,7-Triazacyclononane) with Bromine, Iodine, and Nitric Acid. Syntheses of Air-Stable Hydridocarbonyl and Hydridonitrosyl Complexes. Crystal Structure of $[LMo(CO)_3Br](ClO_4)\cdot H_2O$

PHALGUNI CHAUDHURI,[1a] KARL WIEGHARDT,*[1a] YI-HUNG TSAI,[1b] and CARL KRÜGER*[1b]

Received June 2, 1983

$LM(CO)_3$ complexes (L = 1,4,7-triazacyclononane; M = Cr, Mo, W) have been synthesized, and their reactivity toward bromine, iodine, and nitric acid has been investigated. Air-stable water-soluble cationic complexes $[LM(CO)_3X]^+$ (X = Br, I; M = Mo, W) have been isolated from the reaction with bromine or iodine, whereas the reaction with hydrochloric acid affords $[LM(CO)_3H]^+$, the BF_4^- and ClO_4^- salts of which were isolated as crystalline solids. The reaction with HNO_3 yields cationic nitrosyl complexes $[LM(CO)_2(NO)]^+$ (M = Cr, Mo, W) and $[LM(NO)_2Y]^+$ (Y = Br, H); in the presence of cyanide the neutral complex $[LMo(NO)(CN)_3]$ has been isolated. The perchlorate salt, $[LMo(CO)_3Br](ClO_4)\cdot H_2O$, has been characterized by a three-dimensional X-ray diffraction study. The complex crystallizes in the triclinic space group $P\bar{1}$ with $a = 8.375$ (2) Å, $b = 8.610$ (2) Å, $c = 13.122$ (2) Å, $\alpha = 90.68$ (1)°, $\beta = 90.68$ (1)°, $\gamma = 118.24$ (1)°, $V = 833.4$ Å^3, and $Z = 2$. The structure was solved by conventional methods resulting in a final R factor of 0.043 for 2894 independent reflections. The structure consists of seven-coordinate complex cations, perchlorate anions, and one molecule of water of crystallization. The cation adopts a 4:3 piano-stool configuration.

Introduction

Many of the reactions of terdentate ligands with octahedral group 6B metal carbonyls afford simple carbonyl-substituted complexes of general formula $M(CO)_3L$.[2-4] Rather few complexes of this type with saturated nitrogen donor ligands have been reported. If the incoming ligand is a poorer π-acceptor than CO, *fac*-$M(CO)_3L$ (M = Cr, Mo, W) is the expected configuration, as it has been shown for $Mo(CO)_3(dien)$ (dien = diethylenetriamine).[5,6]

In this paper we describe the results of a study of the reactions of $M(CO)_6$ (M = Cr, Mo, W) with 1,4,7-triazacyclononane ([9]aneN_3 = L), a cyclic terdentate nitrogen donor ligand. This cyclic amine coordinates facially in an octahedron and has been shown to form extremely stable complexes with transition metals in different oxidation states.[7] The stability of the complexes is believed to be due largely to the stereorestrictive mode of coordination imposed by this ligand, although there is growing evidence that a pronounced ligand field strength of the ligand is contributing. Thus, it is possible to study the substitution of carbonyl groups by other ligands while retaining the cyclic triamine in the complex. This type of chemistry has also been developed for the more complex ligand tris(1-pyrazolyl)borate—a uninegative tridentate nitrogen donor ligand.[8]

Nyholm et al.[9] have extensively studied halogen oxidations of group 6B metal tricarbonyl–tris(tertiary arsine) complexes. Since analogous halogen oxidations of tricarbonyl complexes containing terdentate saturated nitrogen donor ligands have not been studied in great detail,[4,8] we have also examined the reactions of our $M(CO)_3L$ complexes with bromine and iodine. Seven-coordinate metal(II) complexes of molybdenum and tungsten have been isolated. As these compounds provide examples of the [M(terdentate)(monodentate)$_4$] seven-coordinate stereochemistry,[10] we have determined the crystal structure of $[Mo([9]aneN_3)(CO)_3Br]ClO_4\cdot H_2O$ prepared in this study.

The employment of nitric acid as a preparative reagent for metal nitrosyl compounds has been quite limited.[11] Obviously, nitrosyl complexes containing metals in relatively high oxidation states are produced. However, Piper et al.[12] used nitric acid to produce $C_5H_5Mn(CO)_2(NO)^+$ in low yield from $C_5H_5Mn(CO)_3$. We found that the $M(CO)_3([9]aneN_3)$ (M = Cr, Mo, W) complexes react readily with aqueous HNO_3 in good yields to give $[LM(CO)_2(NO)]^+$, $[LM(NO_2)_2X]^+$, and $[M_2O_5L_2]^{2+}$ where M = Mo or W and X = H or Br.

---

(1) (a) Ruhr-Universität. (b) Max-Planck-Institut für Kohlenforschung.
(2) Chatt, J.; Watson, H. R. *J. Chem. Soc.* **1961**, 4980.
(3) Howell, I. V.; Venanzi, L. M. *Inorg. Chim. Acta* **1969**, *3*, 121.
(4) Dunn, J. G.; Edwards, D. A. *J. Chem. Soc. A* **1971**, 988.
(5) Abel, E. W.; Bennett, M. A.; Wilkinson, G. *J. Chem. Soc.* **1959**, 2323.
(6) Cotton, F. A.; Wing, R. M. *Inorg. Chem.* **1965**, *4*, 314.
(7) (a) Zompa, L. J.; Young, R. *Inorg. Chem.* **1976**, *15*, 1499. (b) Wieghardt, K.; Küppers, H. J.; Herrmann, W. *Ibid.* **1983**, *22*, 2953.
(8) Trofimenko, S. *J. Am. Chem. Soc.* **1969**, *91*, 588; *Acc. Chem. Res.* **1971**, *4*, 17; *Inorg. Chem.* **1979**, *18*, 2675.
(9) Nyholm, R. S.; Snow, M. R.; Stiddard, M. H. B. *J. Chem. Soc.* **1965**, 6570.
(10) Drew, M. G. B. *Prog. Inorg. Chem.* **1977**, *23*, 67.
(11) Caulton, K. G. *Coord. Chem. Rev.* **1975**, *14*, 317.
(12) Piper, T. S.; Cotton, F. A.; Wilkinson, G. *J. Inorg. Nucl. Chem.* **1955**, *1*, 165.

0020-1669/84/1323-0427$01.50/0 © 1984 American Chemical Society